A NEW TOOL FOR EVALUATING SPECTRAL UNMIXING APPLICATIONS FOR REMOTELY SENSED HYPERSPECTRAL IMAGE ANALYSIS

Luis Ignacio Jimenez, Gabriel Martín and Antonio Plaza

Hyperspectral Computing Laboratory
Department of Technology of Computers and Communications
University of Extremadura, Avda. de la Universidad s/n, E-10003 Caceres, SPAIN
E-mail: lujimenez, gamahefpi, aplaza@unex.es

KEY WORDS: Hyperspectral imaging, spectral unmixing, benchmarking tool, open source implementations

ABSTRACT:

Hyperspectral imaging is a new technique in remote sensing that collects hundreds of images, at different wavelength values, for the same area in the surface of the Earth. For instance, the Airborne Visible Infra-Red Imaging Spectrometer (AVIRIS) instrument operated by NASAs Jet Propulsion Laboratory collects 224 spectral channels in the wavelength range from 40 to 250 nanometers using narrow spectral bands. The new generation of satellite hyperspectral instruments improves this spectral resolution even more, providing very detailed spectral information about ground cover materials. However, the spatial resolution of hyperspectral imaging instruments is still in the range of several meters per pixel. As a result, the pixels collected by an imaging spectrometer are likely mixed in nature. Spectral unmixing is a very important tool in remotely sensed hyperspectral data exploitation which aims at estimating the abundance of pure spectral components (called endmembers) in each mixed pixel. During the past years, many algorithms and models have been developed for endmember extraction and abundance estimation in remotely sensed hyperspectral images, thus making spectral unmixing a hot topic in the hyperspectral imaging literature. However, there is no clearly standardized data set for benchmarking the accuracy of spectral unmixing techniques. In this paper we present a novel tool for hyperspectral unmixing that includes most of these techniques. Also the tool includes a database of sinthetic images generated using random fractal patterns and a real dataset obtained by de AVIRIS sensor of the NASA Jet Propulsion Laboratory. The tool is allowed to perform all the steps of the unmixing chain (Estimating the number of endmembers, feature reduction, endmember extraction and linear spectral unmixing) and also allows the result analysis using several metrics such as the spectral angle distance (SAD) and the root mean reconstruction error (RMSE). The developed open-source tool and quantitative comparison of algorithms is expected to be of great interest to both algorithm developers and end-users of spectral unmixing applications.

1 INTRODUCTION

The availability of hyperspectral instruments with a number of spectral bands that exceed the number of spectral mixture components, such as NASA Jet Propulsion Laboratorys Airborne Visible Infrared Imaging Spectrometer (AVIRIS) (Green et al., 1998), has allowed one to cast the unmixing problem. Spectral mixture analysis (also called *spectral unmixing*) has been an alluring exploitation goal from the earliest days of hyperspectral remote sensing (Goetz et al., 1985) to our days (Plaza et al., 2009). No matter the spatial resolution, the spectral signatures collected in natural environments are invariably a mixture of the signatures of the various materials found within the spatial extent of the ground instantaneous field view of the imaging instrument (Adams et al., 1986). The availability of hyperspectral imagers with a number of spectral bands that exceeds the number of spectral mixture components (Green et al., 1998) has allowed to cast the unmixing problem in terms of an over-determined system of equations in which, given a set of pure spectral signatures (called *endmembers*), the actual unmixing to determine apparent pixel *abundance fractions* can be defined in terms of a numerical inversion process (Keshava and Mustard, 2002). Spectral unmixing has been a very active research area in recent years, since it faces important challenges (Plaza et al., 2011a).

Linear spectral unmixing (Settle and Drake, 1993) is a standard technique for spectral mixture analysis that infers a set of pure spectral signatures, called *endmembers* (Plaza et al., 2004, Du et al., 2008), and the fractions of these endmembers, called *abundances* (Heinz and Chang, 2001), in each pixel of the scene. This model assumes that the spectra collected by the imaging spectrometer can be expressed in the form of a linear combination of endmembers, weighted by their corresponding abundances. Because each observed spectral signal is the result of an actual mixing process, it is expected that the driving abundances satisfy two constraints, i.e., they should be non-negative (Chang and Heinz, 2000), and the sum of abundances for a given pixel should be unity (Chang, 2003). Although the linear model has practical advantages, such as ease of implementation and flexibility in different applications, nonlinear unmixing describes mixed spectra (in physical (Borel and Gerstl, 1994, Liu and Wu, 2004), or statistical (Raksuntorn and Du, 2010) sense) by assuming that part of the source radiation is multiply scattered before being collected at the sensor. The distinction between linear and nonlinear unmixing has been widely studied in recent years. In this work, we focus on linear spectral unmixing due to its simplicity and ease of implementation (Plaza et al., 2011b).

Several algorithms have been developed over the last decade for automatic or semiautomatic extraction of spectral endmembers directly from the input scene. Classic techniques include the orthogonal subspace projection (OSP) (Harsanyi and Chang, 1994), N-FINDR (Winter, 2003), or vertex component analysis (VCA) (Nascimento and Bioucas-Dias, 2005), among many others , but only a few techniques have included the spatial information. For instance, extended morphological operations have been used as a baseline to develop an automatic morphological endmember extraction algorithm (Plaza et al., 2002) for spatialspectral endmember extraction (AMEE). Another spatialspectral approach includes spatial averaging of spectrally similar endmember candidates found via singular value decomposition, called SSEE algorithm (Rogge et al., 2007). Recently, a spatial preprocessing (SPP) algorithm (Zortea and Plaza, 2009) has been proposed, which estimates, for each pixel vector in the scene, a spatially derived factor that is

used to weigh the importance of the spectral information associated to each pixel in terms of its spatial context. The SPP is intended as a preprocessing module that can be used in combination with an existing spectral-based endmember extraction algorithm.

In this paper, we present a first significant effort towards the adoption of a standardized system for evaluating new spectral unmixing applications. The proposed tool, called HyperMix, has been developed using Orfeo Toolbox (http://orfeo-toolbox.org/otb), an open-source library of image processing algorithms. The tool includes a database of synthetic hyperspectral images (using fractals to simulate natural patterns) which can be used to evaluate the precision of several algorithms for endmember extraction and abundance estimation which are already incorporated in the tool. Also, the tool incorporates real hyperspectral image data sets and spectral libraries allowing a detailed quantitative evaluation of algorithm analysis accuracy using metrics based on spectral distances (for evaluating the quality of extracted endmembers), and reconstruction criteria (for evaluating the accuracy of abundance estimation) using an easy-to-use interface which comprises the most relevant techniques for endmember extraction and abundance estimation in the literature. As an innovative contribution of our work, we present an exhaustive inter-comparison of algorithms for endmember extraction and abundance estimation using the considered tool, covering the most recent developments in the field and establishing a quantitative and comparative assesment of algorithms in terms of algorithm precision and computational efficiency using both synthetic and real hyperspectral data sets.

The remainder of the paper is structured as follows. Section 2 describes the proposed tool. Section 3 contains the results obtained with the tool for the fractals image database. Section 4 describes the results obtained for a real hyperspectral dataset. Finally, section 5 concludes the paper with some remarks and hints at plausible future research lines.

2 THE HYPERMIX TOOL

The HyperMix tool includes several algorithms that allows to perform the complete unmixing chain. In the 1 we can see a flowchart of the linear spectral unmixing chain. The linear spectral unmixing chain can be described in four steps: the first step is the estimation of the number of endmembers, then in order to work with less amount of data we can perform an optional feature reduction step, after that we can perform the endmember extraction step and finally the abundances map estimation. In order to perform the estimation of the number of endmembers the HyperMix tool includes the virtual dimensionality (VD) concept (Chang and Du, 2004) and the hyperspectral signal subspace estimation (HySime) algorithm (Bioucas-Dias and Nascimento, 2008). These two methods are the more popular for endmember estimation in the literature. In order to perform the feature reduction step the HyperMix tool include the principal component transform (PCT) (Richards and Jia, 2006) which transform the data space into another which order the components maximizing the data variance.

We can divide the endmember extraction methods available in HyperMix in two groups. In one hand we have the endmembers extraction methods that takes into account the spatial information of the image, on the other hand we have the endmember extraction methods that only uses the spectral pixel's features. The HyperMix tool includes some algorithms in both groups. In the group of algorithms that includes the spatial information we have the AMEE (Plaza et al., 2002), SSEE (Rogge et al., 2007) and SPP (Zortea and Plaza, 2009) algorithms. The SPP has the particularity that it can be combined with any other endmember extraction method, because it has been designed to be a preprocessing module which produces a new dataset as output. The AMEE uses the mophological operations defined over the hyperspectral image in order to search locally the most pure components. The SSEE algorithm first search pure candidate pixels and then average those pixels that are spectrally and spatially related. Both AMEE and SSEE combines the spatial and spectral information in the endmember extraction process. In the other hand we have the endmembers extraction algorithms that only uses the spectral information, these are: NFINDR(Winter, 2003), OSP (Harsanyi and Chang, 1994), VCA (Nascimento and Bioucas-Dias, 2005) and IEA. The NFINDR algorithm tries to find the set of pixels that defines the simplex with highest volume, OSP tries to find a set of signatures orthogonal between them, VCA exploits the fact that the proyection of a simplex in a convex cone is also a simplex, IEA selects iteratively as endmembers those pixels with higher error after reconstruct the image.

In orther to perform the spectral unmixing the HyperMix tool includes the most popular linear spectral unmixing techniques in the literature, these are the unconstrained linear spectral unmixing (LSU), the nonnegative constrained linear spectral unmixing (NCLS) (Chang and Heinz, 2000), the sum to one constrained linear spectral unmixing (SCLS) and the fully constrained linear spectral unmixing (FCLSU) (Heinz and Chang, 2001). LSU solve the linear spectral unmixing problem without impossing any constraint. The NCLS impose the nonnegative constraint which enforces the abundances to be grather or equal than zero. The SCLS impose the sum to one constraint, which simply enforces the abundances of each pixel to sum one. Finally the FCLSU impose both constraints, the sum to one constraint and the positivity constraint at the same time.

The HyperMix tool is designed to be easy to use. The tool includes a graphical interface with a main menu in which you can choose the algorithm to perform. Also the user interfaces includes several displays. One display show the image data, in the second display we can see the abundances map calculated after the unmixing and the third display shows the endmembers. Fig. 2 provides a screenshoot of the HyperMix tool.

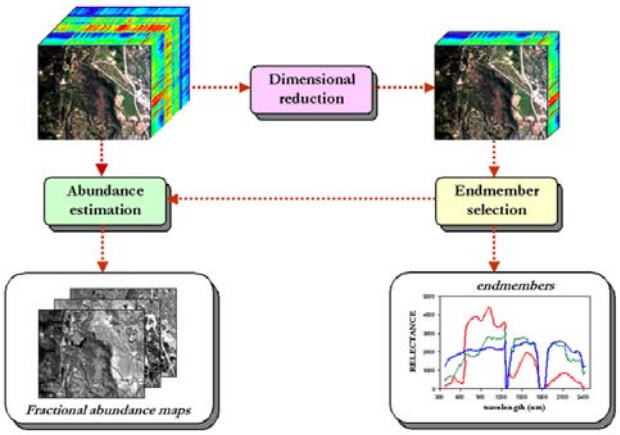

Figure 1: Linear Spectral Unmixing Chain

3 USING HYPERMIX WITH SYNTHETIC HYPERSPECTRAL DATA

A database of 100×100-pixel synthetic hyperspectral scenes created using fractals to generate distinct spatial patterns has been

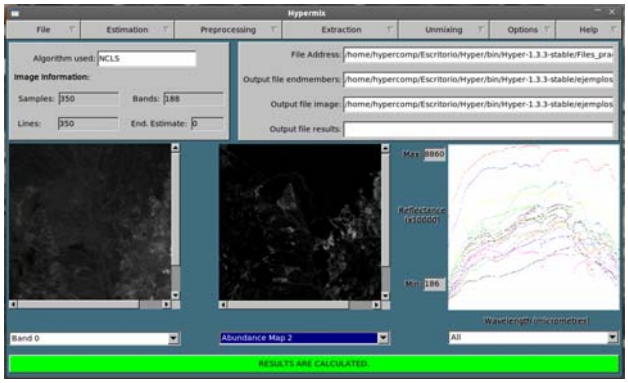

Figure 2: Screenshot of the HyperMix tool after unmixing the AVIRIS Cuprite data set.

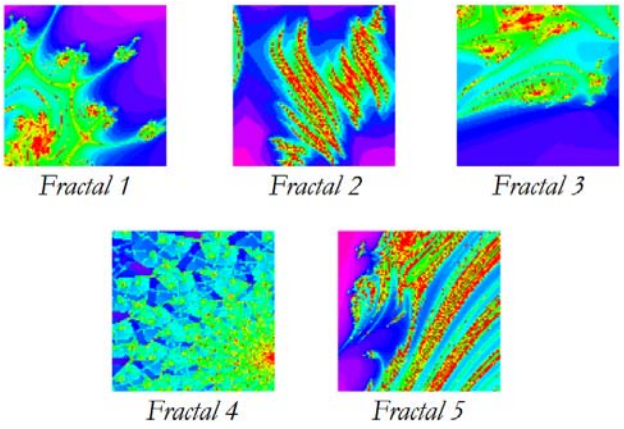

Figure 3: Fractal images used to generate spatial patterns in the generated synthetic images.

included in the HyperMix tool to allow quantitative evaluation of spectral unmixing techniques using this tool. Fig. 3 shows the fractal patterns used to generate the data. The reason for using fractals is that several natural objects can be approximated by fractals to a certain degree, including clouds, mountain ranges, coastlines, vegetables, etc. thus providing a baseline for simulating spatial patterns often found in nature. The synthetic images are simulated from linear mixtures of a set of endmember signatures randomly selected from a spectral library compiled by the U.S. Geological Survey (USGS)[1] and made up of a total of 420 signatures. These images are further divided into a number of clusters using the k-means algorithm (Hartigan and Wong, 1979), where the number of clusters extracted from the five fractal images was always larger than the number of endmember signatures, fixed in our experiments to nine endmembers per scene. The abundance proportions in the regions associated to each cluster have been set so that pixels closer to the border of the region are more heavily mixed, while the pixels located at the center of the region are more spectrally pure in nature (the images does not contain any completely pure pixels, a situation often encountered in real-world analysis scenarios). Zero-mean Gaussian noise was added to the synthetic scenes in different signal to noise ratios (SNRs) –from 30:1 to 110:1– to simulate contributions from ambient and instrumental sources, following the procedure described in (Harsanyi and Chang, 1994). The full database of synthetic scenes has been included in the HyperMix tool but also is available online[2].

[1] http://speclab.cr.usgs.gov/spectral-lib.htm

[2] http://www.umbc.edu/rssipl/people/aplaza/fractals.zip

The metric used to compare the performance of endmember identification algorithms in this work is the spectral angle (Keshava and Mustard, 2002) between each extracted endmember and the set of available USGS ground-truth spectral signatures. The lowest the spectral angle, the better the results. Table 1 shows the average spectral angle scores (in degrees) between the reference USGS mineral spectra and their corresponding endmember pixels produced by several endmember extraction algorithms included in HyperMix, across the considered synthetic scenes. As shown by Table 1, the OSP and VCA (based on spectral information alone) generally provided the best result in the comparison, although the inclusion of spatial information through SPP helped improving the results in some particular cases.

4 USING HYPERMIX WITH REAL HYPERSPECTRAL DATA

We have also used the HyperMix tool to analyze the well-known AVIRIS Cuprite data set, available online in reflectance units[3] after atmospheric correction. This scene has been widely used to validate the performance of endmember identification algorithms. The portion used in experiments corresponds to a 350×350-pixel subset of the sector labeled as f970619t01p02_r02_sc03.a.rfl in the online data. The scene comprises 224 spectral bands between 0.4 and 2.5 μm, with full width at half maximum of 10 nm and spatial resolution of 20 meters per pixel. Prior to the analysis, several bands were removed due to water absorption and low SNR in those bands, leaving a total of 192 reflectance channels to be used in the experiments. Fig. 2 shows an example of processing the AVIRIS Cuprite image with HyperMix. The Cuprite site is well understood mineralogically (Swayze et al., 1992), and has several exposed minerals of interest included in the USGS spectral library. A few selected spectra from the USGS library, corresponding to highly representative minerals in the Cuprite mining district, are used in this work to substantiate endmember signature purity.

Table 2 tabulates the spectral angle scores (in degrees) obtained after comparing the USGS library spectra of *alunite*, *buddingtonite*, *calcite*, *kaolinite* and *muscovite*, with the corresponding endmembers extracted by different algorithms from the AVIRIS Cuprite scene. As in the case of synthetic image experiments, the input parameters of the different algorithms have been carefully optimized so that the best performance for each method is reported in Table 2. For reference, the mean spectral angle values across all five USGS signatures is also reported in Table 2. The number of endmembers to be extracted was set to 19 in all experiments after the consensus reached between the virtual dimensionality (Chang and Du, 2004) and the hyperspectral signal identification by minimum error (HySime) (Bioucas-Dias and Nascimento, 2008) concepts. As shown by Table 2, the best performance (in terms of spectral angle) was obtained by algorithms including both spatial and spectral information simultaneously, such as the AMEE or SSEE.

5 CONCLUSIONS AND FUTURE WORK

In this paper, we have presented a new open-source tool which contains a variety of algorithms for spectral unmixing of remotely sensed data sets. It also comprises a data base of synthetic imagery that can be used to validate new algorithms. The developed open-source tool and quantitative comparison of unmixing algorithms is expected to be of great interest to both algorithm developers and end-users of spectral unmixing applications. In

[3] http://aviris.jpl.nasa.gov/html/aviris.freedata.html

addition to the inclusion of additional techniques for endmember selection, in future work we are planning to incorporate more tools for results analisys and evaluation. Further, we are planning to include efficient implementations in the proposed system that can take advantage of high performance computing systems, such as commodity graphics processing units (GPUs), to accelerate the techniques currently available in HyperMix.

REFERENCES

Adams, J. B., Smith, M. O. and Johnson, P. E., 1986. Spectral mixture modeling: a new analysis of rock and soil types at the Viking Lander 1 site. Journal of Geophysical Research 91, pp. 8098–8112.

Bioucas-Dias, J. M. and Nascimento, J. M. P., 2008. Hyperspectral subspace identification. IEEE Transactions on Geoscience and Remote Sensing 46(8), pp. 2435–2445.

Borel, C. C. and Gerstl, S. A. W., 1994. Nonlinear spectral mixing model for vegetative and soil surfaces. Remote Sensing of Environment 47(3), pp. 403–416.

Chang, C.-I., 2003. Hyperspectral Imaging: Techniques for Spectral Detection and Classification. Kluwer Academic/Plenum Publishers: New York.

Chang, C.-I. and Du, Q., 2004. Estimation of number of spectrally distinct signal sources in hyperspectral imagery. IEEE Transactions on Geoscience and Remote Sensing 42(3), pp. 608–619.

Chang, C.-I. and Heinz, D., 2000. Constrained subpixel target detection for remotely sensed imagery. IEEE Transactions on Geoscience and Remote Sensing 38, pp. 1144–1159.

Du, Q., Raksuntorn, N., Younan, N. H. and King, R. L., 2008. End-member extraction for hyperspectral image analysis. Applied Optics 47, pp. 77–84.

Goetz, A. F. H., Vane, G., Solomon, J. E. and Rock, B. N., 1985. Imaging spectrometry for Earth remote sensing. Science 228, pp. 1147–1153.

Green, R. O., Eastwood, M. L., Sarture, C. M., Chrien, T. G., Aronsson, M., Chippendale, B. J., Faust, J. A., Pavri, B. E., Chovit, C. J., Solis, M. et al., 1998. Imaging spectroscopy and the airborne visible/infrared imaging spectrometer (AVIRIS). Remote Sensing of Environment 65(3), pp. 227–248.

Harsanyi, J. C. and Chang, C.-I., 1994. Hyperspectral image classification and dimensionality reduction: An orthogonal subspace projection. IEEE Transactions on Geoscience and Remote Sensing 32(4), pp. 779–785.

Hartigan, J. A. and Wong, M. A., 1979. Algorithm as 136: A k-means clustering algorithm. Journal of the Royal Statistical Society, Series C (Applied Statistics) 28, pp. 100–108.

Heinz, D. and Chang, C.-I., 2001. Fully constrained least squares linear mixture analysis for material quantification in hyperspectral imagery. IEEE Transactions on Geoscience and Remote Sensing 39, pp. 529–545.

Keshava, N. and Mustard, J. F., 2002. Spectral unmixing. IEEE Signal Processing Magazine 19(1), pp. 44–57.

Liu, W. and Wu, E. Y., 2004. Comparison of non-linear mixture models. Remote Sensing of Environment 18, pp. 1976–2003.

Nascimento, J. M. P. and Bioucas-Dias, J. M., 2005. Vertex component analysis: A fast algorithm to unmix hyperspectral data. IEEE Transactions on Geoscience and Remote Sensing 43(4), pp. 898–910.

Plaza, A., Benediktsson, J. A., Boardman, J., Brazile, J., Bruzzone, L., Camps-Valls, G., Chanussot, J., Fauvel, M., Gamba, P., Gualtieri, J., Marconcini, M., Tilton, J. C. and Trianni, G., 2009. Recent advances in techniques for hyperspectral image processing. Remote Sensing of Environment 113, pp. 110–122.

Plaza, A., Du, Q., Bioucas-Dias, J., Jia, X. and Kruse, F., 2011a. Foreword to the special issue on spectral unmixing of remotely sensed data. IEEE Transactions on Geoscience and Remote Sensing 49(11), pp. 4103–4110.

Plaza, A., Martin, G., Plaza, J., Zortea, M. and Sanchez, S., 2011b. Recent developments in spectral unmixing and endmember extraction. In: S. Prasad, L. M. Bruce and J. Chanussot (eds), Optical Remote Sensing, Springer-Verlag, Berlin, Germany, chapter 12, pp. 235–267.

Plaza, A., Martinez, P., Perez, R. and Plaza, J., 2002. Spatial/spectral endmember extraction by multidimensional morphological operations. IEEE Transactions on Geoscience and Remote Sensing 40(9), pp. 2025–2041.

Plaza, A., Martinez, P., Perez, R. and Plaza, J., 2004. A quantitative and comparative analysis of endmember extraction algorithms from hyperspectral data. IEEE Transactions on Geoscience and Remote Sensing 42(3), pp. 650–663.

Raksuntorn, N. and Du, Q., 2010. Nonlinear spectral mixture analysis for hyperspectral imagery in an unknown environment. IEEE Geoscience and Remote Sensing Letters 7(4), pp. 836–840.

Richards, J. A. and Jia, X., 2006. Remote Sensing Digital Image Analysis: An Introduction. Springer.

Rogge, D. M., Rivard, B., Zhang, J., Sanchez, A., Harris, J. and Feng, J., 2007. Integration of spatial–spectral information for the improved extraction of endmembers. Remote Sensing of Environment 110(3), pp. 287–303.

Settle, J. J. and Drake, N. A., 1993. Linear mixing and the estimation of ground cover proportions. International Journal of Remote Sensing 14, pp. 1159–1177.

Swayze, G., Clark, R. N., Kruse, F., Sutley, S. and Gallagher, A., 1992. Ground-truthing AVIRIS mineral mapping at Cuprite, Nevada. Proc. JPL Airborne Earth Science Workshop pp. 47–49.

Winter, M. E., 2003. N-FINDR: an algorithm for fast autonomous spectral end-member determination in hyperspectral data. Proc. SPIE Image Spectrometry V 3753, pp. 266–277.

Zortea, M. and Plaza, A., 2009. Spatial preprocessing for endmember extraction. IEEE Transactions on Geoscience and Remote Sensing 47, pp. 2679–2693.

Table 1: Average spectral angle scores (in degrees) between the USGS mineral spectra and their corresponding endmembers produced by several endmember selection algorithms available in HyperMix.

Algorithm	**SNR=30:1**	**SNR=50:1**	**SNR=70:1**	**SNR=90:1**	**SNR=110:1**
N-FINDR	2.095	0.463	0.383	0.388	0.361
OSP	2.118	0.452	0.349	0.361	0.345
VCA	1.193	0.467	0.377	0.430	0.426
IEA	3.036	1.048	0.825	0.688	1.325
SPP+N-FINDR	2.293	0.778	0.701	0.694	0.693
SPP+OSP	2.342	0.622	0.536	0.529	0.529
SPP+VCA	2.271	0.455	0.327	0.319	0.347
SPP+IEA	3.958	1.723	1.579	1.357	1.607
AMEE	2.670	1.260	0.969	1.193	1.252
SSEE	2.124	1.077	0.576	0.722	0.645

Table 2: Spectral angle scores (in degrees) between USGS mineral spectra and their corresponding endmembers produced by several endmember selection algorithms available in HyperMix.

Algorithm	**Alunite GDS84**	**Buddingtonite GDS85**	**Calcite WS272**	**Kaolinite KGa-1**	**Muscovite GDS107**	**Mean**
N-FINDR	4.81	4.29	7.60	9.92	5.05	6.33
OSP	4.81	4.16	9.52	10.76	5.29	6.91
VCA	6.91	5.38	9.53	9.65	6.47	7.59
IEA	4.81	6.03	5.93	11.14	7.91	7.17
SPP+N-FINDR	7.72	4.27	9.34	11.26	5.69	7.66
SPP+OSP	6.06	4.27	8.43	12.28	4.64	7.14
SPP+VCA	14.11	8.49	11.94	13.86	5.61	10.80
SPP+IEA	5.70	6.34	6.41	15.38	4.64	7.69
AMEE	4.81	4.17	5.87	8.74	4.61	5.64
SSEE	4.81	4.16	8.48	10.73	4.63	6.57